

Regulation and Characterization of Polar Groups on the Surfaces of Cellulose Nanocrystal–Nanosilver Hybrids

Fangfang Lu, Hairong Wang, Liang Li, Kunyu Mao, Jiahao Chen, and Haodi Yue

Cellulose nanocrystals (CNCs) with a high content of polar groups were prepared *via* the oxidation process by controlling the amount of mixed acid, incorporating additional additive of citric acid and vitamin C as active agents, and applying ultrasonic crosslinking. Subsequently, cellulose nanocrystal–silver (CNC–Ag) nanohybrid materials were synthesized *via* an oxidation hydrolysis reaction, which displayed good dispersibility and high interaction, leading to the hydrogen bonding between polar groups (-OH and -COOH) on the surface of CAC–Ag nanohybrids. The positive effects of hydrogen bonding on the surface of CAC–Ag nanohybrids were confirmed by the high carboxyl group content (2.69 mmol/g) and low contact angle (53.7°) tested. In addition, CAC–Ag nanohybrids showed significant antibacterial activity against both Gram-negative *E. coli* and Gram-positive *S. aureus*. These results showed that the high-performance CNC–Ag nanohybrids prepared in this study may be highly suitable as nano-fillers for polyester materials used in antibacterial food packaging.

DOI: 10.15376/biores.18.4.7700-7712

Keywords: Nanohybrids; Polar groups; Ultrasonic crosslinking; Antibacterial activity

Contact information: Zhoushan Institute of Calibration and Testing for Quality and Technology Supervision, Zhoushan 316000, China; *Corresponding author: 17826854282@163.com

INTRODUCTION

In past decades, the synthesis of biodegradable nanocomposites with organic and inorganic hybrids has been widely reported in food packaging fields, which have potential to replace the plastic products and effectively reduce the white pollution (Yu *et al.* 2015; Lu *et al.* 2016). Thus, some biodegradable polymers, such as poly (3-hydroxybutyrate-co-3-hydroxyvalerate) (PHBV) (Yu *et al.* 2015) are used to prepare high-performance nanocomposites. However, biodegradable nanocomposites often face challenges such as gradual accumulation and additive dispersion when incorporating nanofillers into the polymer matrix. To overcome these challenges, nanoscale hybrids with high surface-to-volume ratios and specific chemical structures were selected to establish strong interactions between the polymer matrix and nanohybrids, resulting in enhanced physicochemical properties of the nanocomposites (Fortunati *et al.* 2012; Ramdani *et al.* 2014; Mane *et al.* 2015; Zhou *et al.* 2019; Chen *et al.* 2020).

Recently, cellulose nanocrystals (CNCs) with various rod-like or spherical shapes isolated from the most abundant cellulosic materials have gained increasing attention in some fields such as antimicrobial packaging (Yu *et al.* 2015; Zhang *et al.* 2017) and templates for metallic nanoparticles (Lu *et al.* 2016). This attention is due to their excellent properties, including easily modified functional groups, high specific area, aspect ratios, and outstanding stiffness. As the nanofillers, the requirement of CNCs surface group varies

with the applications. In Yu's work, the antibacterial activity of thermally stable corn-like cellulose nanocrystal-nanosilver (CNC-Ag) nanohybrid was fabricated by the one-pot green method. Furthermore, in Zhang's work, the research related to the different nanosilver contents in CNC-Ag nanohybrids on PHBV showed that the homogeneously dispersed CNC-Ag with higher nanosilver contents showed stronger heterogeneous nucleation effect than only CNCs on PHBV matrix, which caused obvious improvements for PHBV. There were larger enhancements in the thermal stability, mechanical and antibacterial properties than the pristine PHBV matrix. In general, in the above mentioned reported literature, the nanosilver not only gives the nanocomposite antibacterial properties, but it also acts as a nucleating agent to enhance the integral properties (such as mechanical and thermal) of the nanocomposites. However, in the previously reported literature, CNCs with functional groups (carboxyl groups) were usually prepared with mixed acid solutions of inorganic acids (such as hydrochloric acid and sulfuric acid) and organic acid (formic acid), 2,2,6,6-tetramethylpiperidiny-1-oxyl (TEMPO) (Ganguly *et al.* 2021; Paralikar *et al.* 2008), ammonium persulfate (APS) (Cheng *et al.* 2014), and NaIO₄ oxidations (Lu *et al.* 2016). The preparation process takes a long time. The water bath condition and the oxidizing agents are toxic, and the subsequent waste solution is not friendly to the environment.

Citric acid (CA) is a natural organic acid produced by microbial fermentation (Adeoye and Lateef 2022). It is an organic acid with 3 H₃O⁺ groups. As a weak acid, it is relatively safe to use. In addition, the raw materials for preparing citric acid are derived from food manufacturing, which provides further demonstration of its safety. Compared with inorganic acids, the safety and reliability of CA is favorable. Citric acid will not adversely affect the environment, since it is easy to degrade under the action of microorganisms and heat, and the waste liquid is also relatively easy to handle.

Vitamin C (L-ascorbic acid, AA) is a six-carbon compound with a endol-lactone resonance structure (Mallakpour and Sadeghzadeh 2015). There are two active hydroxyl groups in the structure of lactone ring, which provides strong reducibility and renders it easy to ionize (Berg 2015). AA is easy to react with some other compounds (or atomic groups, metal ions) to increase its own valency, and reduce the valency of other atoms (or atomic groups, metal ions). In other words, ascorbic acid can easily lose electrons in a reaction. AA is essential for life and acts as a strong water-soluble antioxidant. It is mainly derived from fruits and vegetables (Carr and Vissers 2013).

In the present work, CNC-Ag nanohybrids with various polar group contents (-OH and -COOH) on the surfaces were prepared by controlling the CNCs synthesis method, introducing a reducing agent (AA), employing a crosslinking agent (CA), utilizing ultrasonic crosslinking, and applying other experimental conditions. The morphologies, microstructures, and properties of the CNC-Ag nanohybrids were investigated, and their potential application for antibacterial testing was evaluated.

EXPERIMENTAL

Materials

Commercial microcrystalline cellulose (MCC), consisting of ruby-shaped fragments with a particle size from 25 to 30 μm, was purchased from Shanghai Chemical Reagents, China. Sodium periodate (NaIO₄), silver nitrate (AgNO₃), hydrochloric acid

(HCl), formic acid (HCOOH), sulfuric acid (H₂SO₄), ammonia solution (NH₃•H₂O), sodium hydroxide (NaOH), hydroxylamine–hydrochloride (NH₂OH•HCl), citric acid (CA), and ascorbic acid (AA) were purchased from Hangzhou Mike Chemical Agents Co. Ltd., China. These chemical reagents and materials were used as received without further purification, and deionized water (Millipore Milli-Q purification system) was used in the experimental procedures.

Preparation of CNC

Cellulose nanocrystals (CNCs) were prepared *via* a one-step method of mixed acid with a solid-to-liquid ratios of 1:50 [g/mL]. Three specific mixed acid ratios were used: Mixed acid No.1: V_{6M HCl}/V_{6M HCOOH} = 1/9, No.2: V_{6M HCl}/V_{6M HCOOH}/V_{6M CA} = 1:4.5:4.5, No.3: V_{6M HCl}/V_{6M HCOOH}/V_{6M CA} = 1/1.5/7.5. The detailed process was as follows: 1 g of MCC was put into the mixed acid in a 100 mL flask and continuously stirred. After mechanical stirring for 4 h at a reaction temperature of 80 °C, the product was collected *via* centrifugation and freeze-dried for 48 h. The resulting samples were named CNC, CNC (4.5), and CNC (7.5).

Preparation of CNC–Ag Nanohybrids

The synthesis procedures of CNC–Ag nanohybrids are shown in Fig. 1 (Yu *et al.* 2014a,b, 2016).

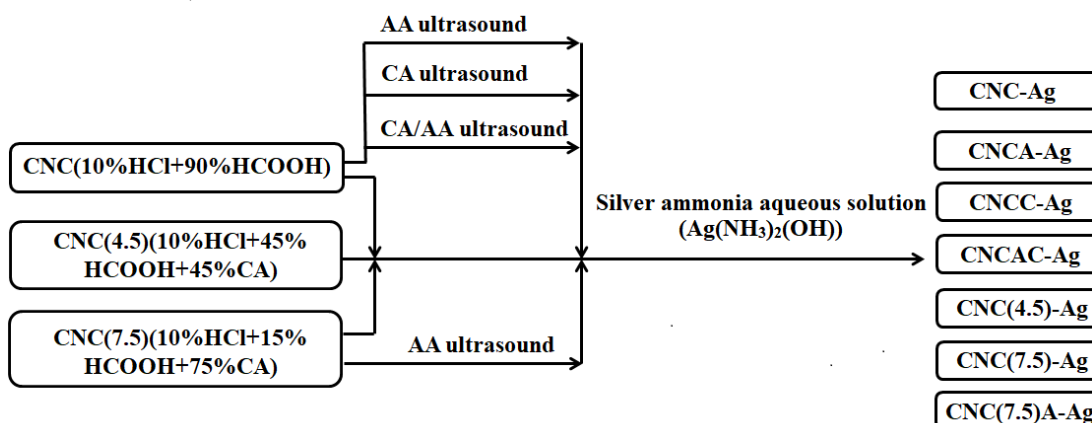


Fig. 1. Preparation flowchart of CNC-Ag nanohybrid materials with different polar groups

Method 1: The silver ammonia aqueous solution (Ag(NH₃)₂(OH)) was prepared by adding 1 mL of 25% ammonia to 100 mL AgNO₃ (0.85 g) solution. The ammonia was added dropwise to obtain a clear solution. Then, the CNs (CNC, CNC (4.5), CNC (7.5)) suspensions (about 1.0 g dry CNs) were heated at a reaction temperature of 90 °C until the color of the solution no longer changed. After cooling at room temperature, the precipitates were washed with deionized water *via* successive centrifugation to remove the residual silver ammonia and the reaction byproducts, and the samples were dried and denoted as CNC-Ag, CNC (4.5)-Ag, and CNC (7.5)-Ag, respectively.

Method 2: Then, 1 g of CNC was weighed and dispersed in water up to a volume of 100 mL in a three-neck round bottom flask. The CA (approximately 6.3 g) and AA (approximately 6.3 g) were added successively with ultrasonic treatment for 30 min. Then, the aforementioned silver ammonia aqueous solution (Method 1) was added dropwise into the CNC mixed suspension under mechanical stirring and ultrasonic treatment until the

color of the solution no longer changed under the room temperature. The reaction was shielded from light, and the hybrid materials obtained were named CNCA–Ag, CNCC–Ag, and CNCAC–Ag.

Method 3: Then, 1g of CNC (7.5) was weighed and dispersed in water up to a volume of 100 mL in a three-neck round bottom flask. AA ~ 6.3 g was added with ultrasonic treatment for 30 min. Then the aforementioned silver ammonia solution (Method 1) was added dropwise into the CNC (7.5) mixed suspension under mechanical stirring and ultrasonic treatment until the color of the solution no longer changed. The reaction was shielded from light, and the hybrid material obtained was named CNC (7.5) A–Ag.

PHBV/CNC–Ag Composites Processing

PHBV/CNC–Ag composites were prepared by solvent-casting technique (Yu *et al.* 2014a). First, CNC–Ag nanohybrid materials were dissolved in CHCl₃ (10%, wt/v) with vigorous stirring at room temperature. The well dispersed 10 wt% CNC–Ag nanohybrids suspension in CHCl₃ was slowly dropped into PHBV solution in CHCl₃. The mixture was cast on a glass slide. After the solvent was evaporated completed at room temperature, nanocomposite films with a thickness of 70 to 80 μm were obtained. All films were placed in a vacuum oven at 40 °C for 2 weeks before characterization to remove residual chloroform.

Determination of the Carboxyl Group Content

The carboxyl group content of CNC–Ag nanohybrids was determined *via* conductimetric titration. Conductimetric titration involves the addition of a salt base into an acid, using sodium hydroxide standard solution *via* conductimetric titration under a neutral salt environment. The conductivity was measured as the ordinate, and the volume of NaOH consumed (mL) was measured as the abscissa. The carboxyl group content of the CNC–Ag nanohybrids were calculated based on the turning point in the curve. The carboxyl group content of the sample (COOH⁻, mmol/g) was calculated using Eq. 1,

$$[\text{COOH}^-] = (M \times V)/W \quad (1)$$

where *M* is the concentration of the NaOH standard solution (M/L), *V* is the NaOH standard solution volume (mL) corresponding to the turning point and *W* is the weight of CNC–Ag nanohybrids (g).

Characterization

The morphologies of the CNC–Ag were observed using field-emission scanning electron microscopy (FE-SEM, JSM-5610; JEOL, Japan) at an acceleration voltage of 1.0 kV at room temperature.

The chemical structure of the samples was analyzed using a Nicolet 5700 FTIR spectrometer.

The optical properties of the CNC–Ag nanohybrids were analyzed with a UV–Vis spectrophotometer. Measurements were within a wavelength range from 200 to 900 nm.

Gram-negative *Escherichia coli* (*E. coli*) and Gram-positive *Staphylococcus aureus* (*S. aureus*) were chosen to investigate the antimicrobial activities of PHBV/CNC–Ag composites, and the detailed procedure was as follows (Yu *et al.* 2015; Zhang *et al.* 2017): The antibacterial properties of PHBV nanocomposites were determined via qualitative and quantitative experiments. For the qualitative experiment, the PHBV

nanocomposites (made into a disc shape with the diameter of 1.0 cm) were evaluated against *E. coli* and *S. aureus*. The columnar gels (made by 10 g sodium chloride, 15 g agar, 5 g yeast extract powder, and 5 g peptone in 1L distilled water under high pressure and temperature using a sterilization pot) were placed on the culture dishes which coated with *E. coli* and cultured at 37 °C for 24 h for the detection of inhibition zone.

In addition, for the quantitative experiment, the antibacterial ratio (AR) was calculated by counting the mean colony forming units (CFU), which could be achieved by manually counting the number of viable microorganism colonies under incubation the plates at 37 °C for 24 h. These results were multiplied by the dilution factor, and the duplicate counts were averaged. The antibacterial ratio of these samples was determined by the following equation,

$$\text{Antibacterial ratio (\%)} = (N_0 - N) / N_0 \quad (2)$$

where N_0 is the mean number of bacteria on neat PLA film samples (CFU/sample), and N is the mean number of bacteria on the PHBV nanocomposites samples (CFU/sample). Five replicates were performed and the average values were reported.

RESULTS AND DISCUSSION

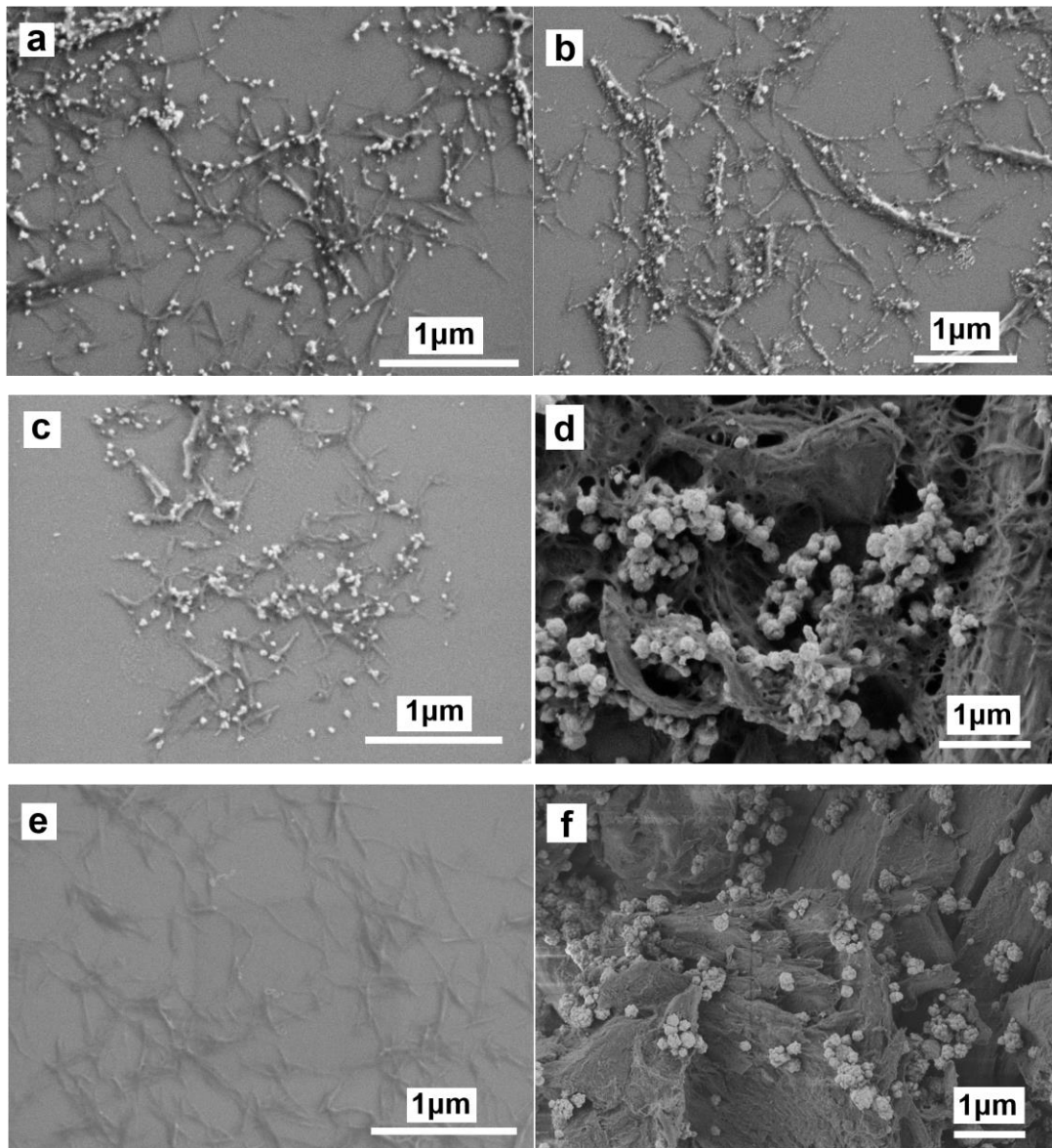
Morphology

The morphologies of CNC–Ag nanohybrids and the silver nanoparticles with spherical shapes on their surfaces were uniformly distributed with average diameters of 28.5, 37, and 40.5 nm for CNC–Ag, CNC (4.5)–Ag, and CNC (7.5)–Ag, respectively (Fig. 2a–c). This indicated that the redox reaction between the silver ions from the silver ammonia aqueous solution and the methyl ester group on the surface of CNC could generate uniformly distributed silver nanoparticles on the surfaces of CNC–Ag. As a result, the methyl ester groups generated on the surface of CNC, and each ester group contained an aldehyde group, which could be able to reduce Ag^+ into Ag^0 that would diffuse and aggregate into nanoparticles directly on the surfaces of CNC (Yu *et al.* 2013). The reaction was relatively mild without the addition of an additional reducing agent (AA). Additionally, the slight difference in silver nanoparticles sizes between CNC–Ag, CNC (4.5)–Ag, and CNC (7.5)–Ag was attributable to the different methyl ester group content on their surfaces.

In Fig. 2 d, the size of spherical silver nanoparticles attached on the surface of CNCA–Ag was 80.5 nm, suggesting that the addition of AA to the reaction system accelerated the reduction of silver ions to silver nanoparticles under ultrasonic conditions at room temperature. However, the size of silver nanoparticles gradually aggregated into larger particles due to a lack of dispersants, such as polyvinyl pyrrolidone (PVP) and ethylene glycol ester, to protect the silver nanoparticles generated by the redox reaction.

In Fig. 2 e, under ultrasonic conditions at room temperature, silver ions were not reduced to silver nanoparticles without the addition of AA to the reaction system, and the sample was named CNCC–Ag. With the successive addition of AA and CA in the reaction at room temperature (Fig. 2 f), silver nanoparticles were generated with an average diameter of 150.3 nm. Comparing the size of silver nanoparticles on CNCA–Ag (reaction time of 30 min) with CNCA–Ag (reaction time of 60 min) indicated that the prolonged reaction time resulted in the continuous or gradual assembly of silver nanoparticles into larger particles.

In Fig. 2 g, CNC (7.5) AC–Ag shows that with CA in the reaction system and the highest carboxyl group content on the surface of CNC (7.5), was due to the largest proportion of CA in the mixed acid used in the preparation of CNC samples. As a result, larger silver nanoparticles with an average diameter of 131.5 nm were formed on the surface of CNC (7.5) AC–Ag. Compared with CNCA–Ag, and CNC (7.5) AC–Ag, the diameter of silver nanoparticles increased with the enhancement of carboxyl group content on the CNC surface under the same reaction conditions at room temperature.



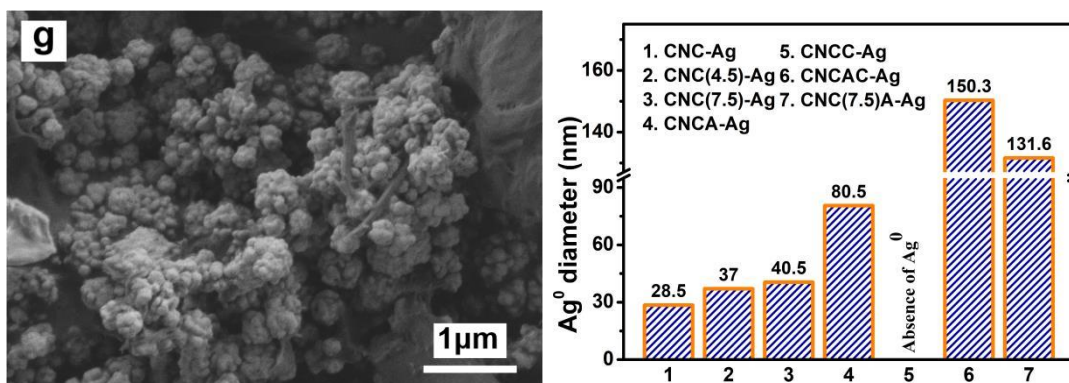


Fig. 2. FE-SEM micrographs of CNC-Ag(a), CNC(4.5)-Ag(b), CNC(7.5)-Ag(c), CNCA-Ag(d), CNCC-Ag(e), CNCAC-Ag(f), CNC(7.5)A-Ag(g), and nanometer nanosilver size summary diagram

FT-IR Spectra Analysis

The FT-IR spectra of CNC-Ag nanohybrids are shown in Fig. 3. The peaks at 1725 cm^{-1} with different intensities were assigned to the carbonyl groups (C=O), which belong to the carboxyl groups (-COOH) of CA (Ghezelbash *et al.* 2012), CNC (4.5)-Ag, CNC (7.5)-Ag, CNCC-Ag, CNCAC-Ag, and CNC (7.5)A-Ag nanohybrids. Additionally, the absorbance at 1630 cm^{-1} confirmed the presence of AA on the surface of CNC-Ag nanohybrids (Mallakpour and Sadeghzadeh 2015). Furthermore, according to the spectra, different mixed acid ratios did not change the chemical structure of CNC. Thus, the CNC-Ag nanohybrids retained the original chemical structure of CNC while incorporating polar groups (-OH, -COOH) introduced by CA and AA.

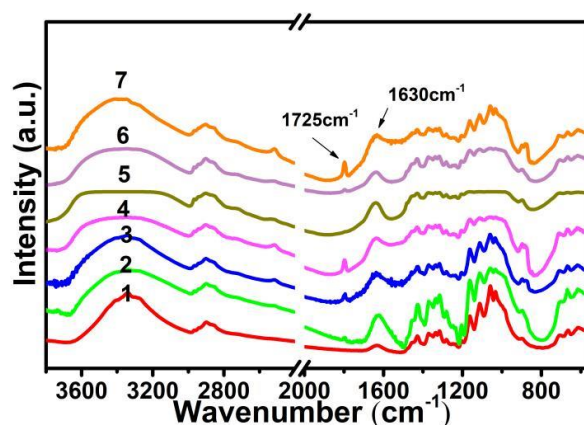


Fig. 3. FT-IR spectra of CNC-Ag (1), CNC(4.5)-Ag(2), CNC(7.5)-Ag(3), CNCA-Ag(4), CNCC-Ag(5), CNCAC-Ag(6), CNC(7.5)A-Ag(7) nanohybrids

Carboxyl Group Content and Contact Angle

Figure 4 shows the carboxyl group content of CNC-Ag (0.24 mmol/g) and CNCA-Ag (0.29 mmol/g), which were relatively lower compared with CNC (4.5)-Ag, CNC (7.5)-Ag, CNCC-Ag, CNCAC-Ag, and CNC (7.5)A-Ag (2.02–2.69 mmol/g). Compared with CNC-Ag and CNCA-Ag, the preparation process for CNC was same (Mixed acid No.1: $V_{6M\text{ HCl}} / V_{6M\text{ HCOOH}} = 1/9$), and the slight difference in carboxyl group content was due to the interaction between the AA and the hydrogen bonding on the surface of CNC-Ag

during ultrasonic cross-linking. This interaction helped reduce the loss of carboxyl group content during preparation of the nanohybrids. Additionally, the difference in the carboxyl group content of CNC–Ag (0.24 mmol/g), CNC (4.5)–Ag (2.28 mmol/g), and CNC (7.5)–Ag (2.49 mmol/g) was related to the mixed acid ratio used in the CNC preparation methods. CA was not used in the preparation of CNC (4.5)–Ag and CNC (7.5)–Ag.

In comparison to CNCA–Ag (0.29 mmol/g), CNCC–Ag (2.47 mmol/g), and CNCAC–Ag (2.69 mmol/g), the preparation process for CNC was the same (hydrochloric acid/formic acid, v/v = 1:9). The differences in the carboxyl content was due to the absence of CA addition in the CNCA–Ag, and CNCC–Ag reaction system, resulting in relatively lower carboxyl group content on their surfaces. In summary, the addition of CA can increase the carboxyl group content to some extent. For CNCAC–Ag, with the help of ultrasonic treatment, a significant number of carboxyl groups were introduced. The polar groups (-OH and -COOH) from the CA and the hydroxyl group on AA created hydrogen bonding on the surface of CNC, leading to the introduction and fixation of high content on the surface of CNCAC–Ag.

Compared with CNC (7.5)–Ag (2.49 mmol/g) and CNC (7.5)A–Ag (2.02 mmol/g), the CNC raw materials used were the same (mixed acid 3:V_{6M} HCl / V_{6M} HCOOH / V_{6M} CA = 1/1.5/7.5), but the reducing agent (AA) was added to the CNC (7.5)A–Ag system. The resulting nanohybrids contained a large amount of nano-silver on the surfaces, which weakened the hydrogen bonding between polar groups. This led to a lower carboxyl content which anchored by hydroxyl group (-OH) on the CNC (7.5)A–Ag surfaces than CNC (7.5)–Ag. Figure 4 shows the contact angle of CNC–Ag nanohybrid materials, which is often used to evaluate the hydrophilicity of hybrid materials. The larger the carboxyl group content of the nano-hybrid material resulted in a smaller the contact angle. The hydrophilic carboxyl group and the increased hydrophilicity of the nano-hybrid material reduce agglomeration and enhance its compatibility (Yu *et al.* 2014a).

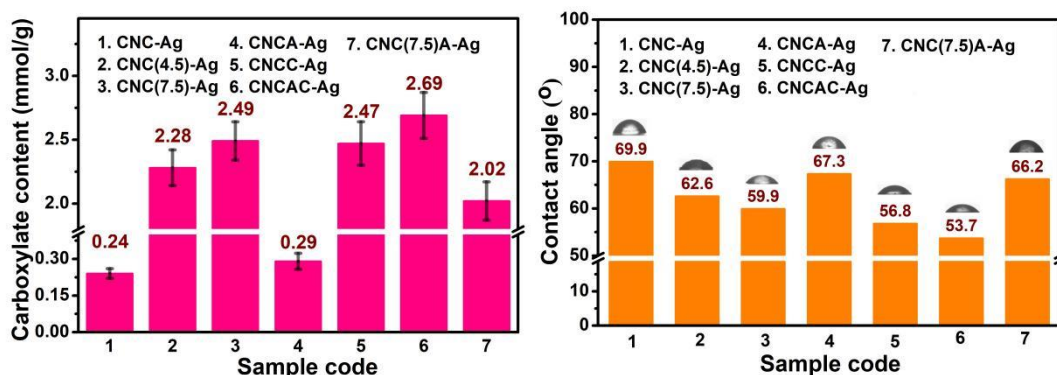


Fig. 4. Carboxyl group content (mmol/g) (a) and contact angle (°) (b) of CNC-Ag nanohybrid materials

UV-vis Absorbance Property

UV-Vis spectroscopy is an important technique for verifying the formation and stability of nanosilver particles (Fig. 5). The color of these particles depends on their size (Awwad *et al.* 2013). The characteristic peak corresponding to nanosilver particles was centered around 420 nm for CNC–Ag, CNC (4.5)–Ag, and CNC (7.5)–Ag. However, a blue shift from ~420 to ~380 nm in the characteristic peak was observed for CNCA–Ag, CNCAC–Ag, and CNC (7.5)A–Ag. This shift is attributed to the increased average length

of the nano-silver particles on the CNC–Ag surface facilitated by the presence of AA (reducing agent) (Sun *et al.* 2002). Additionally, the CNCC-Ag nanohybrids did not show characteristic peaks. This confirmed that the scanning electron microscope images (Fig. 2e) showed obvious silver nanoparticles.

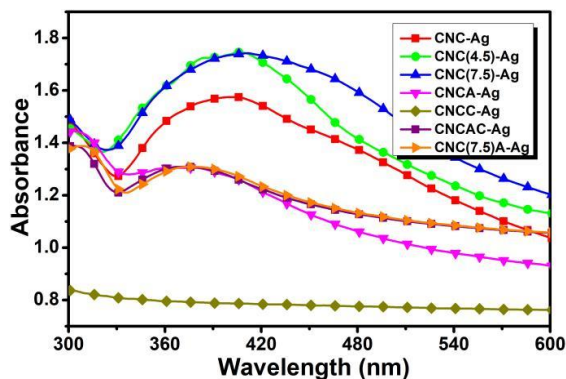


Fig. 5. UV–Vis spectroscopy of CNC-Ag nanohybrid materials

Antibacterial Property

The antibacterial properties of PHBV nanocomposites were determined *via* qualitative and quantitative experiments. Figure 6 shows the bacteriostatic zone of the nanocomposites against *E. coli* and *S. aureus*, which was determined *via* the agar plate method.



Fig. 6. Antibacterial zones for *E.coli* and *S. aureus* of PHBV nanocomposites

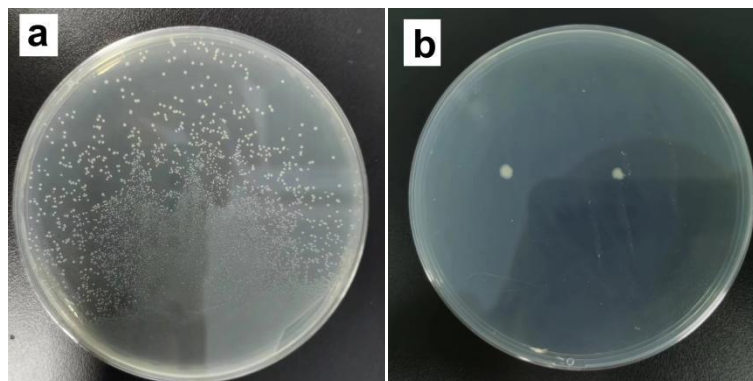


Fig. 7. Antibacterial ratio of pristine PHBV (a) and the PHBV/CNC-Ag (b)

After 12 h of the bacteria culture on the solid medium, the nanocomposite membrane exhibited selective antibacterial activity against *E. coli* and *S. aureus*. The antibacterial effect of the nanocomposite on *S. aureus* was more pronounced compared with *E. coli*. As shown in Fig. 6, the antibacterial zone size of the nanocomposites against *E. coli* ranged from 0.5 to 1 mm, while that for *S. aureus* ranged from 1.1 to 3.6 mm. The PHBV/CNC (7.5)A–Ag exhibited the largest antibacterial zone, reaching up to 3.6 mm against *S. aureus*. The high nanosilver content in PHBV/CNC (7.5)A–Ag imparted a relatively durable antibacterial effect, resulting in the largest antibacterial zone. Furthermore, the antibacterial rate of the nanocomposites was quantitatively analyzed via the vibration method. All nanocomposites exhibited bacterial resistance rates of 97.4 to 100 %.

Table 1. Antibacterial Resistance (AR) Values of PHBV Nanocomposites

AR	PHBV/ CNC–Ag	PHBV/ CNC (4.5)–Ag	PHBV/ CNC (7.5)–Ag	PHBV/ CNCA–Ag
<i>E. coli</i> (%)	99.9	99.5	98.9	97.5
<i>S. aureus</i> (%)	100.0	100.0	99.9	99.9
AR	PHBV/ CNCC–Ag	PHBV/ CNCAC–Ag	PHBV/ CNC (7.5)A–Ag	PHBV
<i>E. coli</i> (%)	97.4	97.5	97.5	/
<i>S. aureus</i> (%)	99.5	99.9	99.9	/

CONCLUSIONS

1. CNC–Ag nanohybrids with different polar groups (-OH and -COOH) content were prepared via redox reaction and the content of polar groups on the surface of CAN–Ag nanohybrids were controlled via the preparation method of CNC, introducing reductant (AA), a crosslinking agent (CA), and ultrasonic crosslinking conditions.
2. CNC–Ag nanohybrids displayed good dispersibility, helping to improve the spatial dispersibility and adhesion properties after blending with other subsequent biopolyesters. The polar groups on the CAN–Ag nanohybrids surface accelerated the effect of hydrogen bonding and interface interaction.

3. CNC-Ag nanohybrids exhibited good antibacterial activities against Gram-negative *Escherichia coli* and Gram-positive *Staphylococcus aureus*.
4. The high-performance CNC–Ag nanohybrids prepared in this study may be highly suitable as nano-fillers for polyester materials used in antibacterial food packaging.

ACKNOWLEDGEMENTS

This work was financially supported by the Fund for Science and Technology Project of Zhoushan (2022C31068).

REFERENCES CITED

- Adeoye, A. O., and Lateef, A. (2022). “Improving the yield of citric acid through valorization of cashew apple juice by *Aspergillus niger*: Mutation, nanoparticles supplementation and Taguchi technique,” *Waste and Biomass Valorization* 13(4), 2195-2206. DOI: 10.1007/s12649-021-01646-0
- Awwad, A. M., Salem, N. M., and Abdeen, A. O. (2013). “Green synthesis of silver nanoparticles using carob leaf extract and its antibacterial activity,” *International Journal of Industrial Chemistry* 4, 1-6. DOI: 10.1186/2228-5547-4-29
- Berg, R. W. (2015). “Investigation of L (+) - ascorbic acid with Raman spectroscopy in visible and UV light,” *Applied Spectroscopy Reviews* 2015(50), 193-239. DOI: 10.1080/05704928.2014.952431
- Carr, A. C., and Vissers, M. C. M. (2013). “Synthetic or food-derived vitamin C are they equally bioavailable,” *Nutrients* 5(11), 4284-4304. DOI: 10.3390/nu5114284
- Chen, J., Yang, R., Ou, J., Tang, C., and Tam, K. C. (2020). “Functionalized cellulose nanocrystals as the performance regulators of poly (β -hydroxybutyrate-co-valerate) biocomposites,” *Carbohydrate Polymers* 242, article 116399. DOI:10.1016/j.carbpol.2020.116399.
- Cheng, M., Qin, Z. Y., Liu, Y. N., Qin, Y. F., Li, T., Chen, L., and Zhu, M. F. (2014). “Efficient extraction of carboxylated spherical cellulose nanocrystals with narrow distribution through hydrolysis of lyocell fibers by using ammonium persulfate as an oxidant,” *Journal of Materials Chemistry A*, 2, 251-258. DOI: 10.1039/C3TA13653A
- Ganguly, K., Patel, D. K., Dutta, S. D., and Lim, K. (2021). “TEMPO-CNC-capped gold nanoparticles for colorimetric detection of pathogenic DNA,” *ACS Omega*, 6, 19, 12424-12431. DOI: 10.1021/acsomega.1c00359
- Ghezelbash, Z., Ashouri, D., Mousavian, S., Ghandi, A. H., and Rahnama, Y. (2012). “Surface modified Al₂O₃ in fluorinated polyimide/ Al₂O₃ nanocomposites: Synthesis and characterization,” *Bulletin of Materials Science* 35(6), 925-931. DOI: 10.1007/s12034-012-0385-4
- Li, H., Yan, Y., Liu, B., Chen, W., and Chen, S. (2007). “Studies of surface functional modification of nanosized α -alumina,” *Powder Technology* 178(3), 203-207. DOI: 10.1016/j.powtec.2007.04.020

- Lu, F. F., Yu, H. Y., Yan, C. F., and Yao, J. M. (2016). "Polylactic acid nanocomposite films with spherical nanocelluloses as efficient nucleation agents: effects on crystallization, mechanical and thermal properties," *RSC Advances* 6(51), 46008-46018. DOI: 10.1039/c6ra02768g
- Mallakpour, S., and Sadeghzadeh, R. (2015). "A benign and simple strategy for surface modification of Al₂O₃ nanoparticles with citric acid and l(+)-ascorbic acid and its application for the preparation of novel poly(vinyl chloride) nanocomposite films," *Advances in Polymer Technology* 36. DOI: 10.1002/adv.21622
- Mane, A. T., Navale, S. T., Pawar, R. C., Lee, C. S., and Patil, V. B. (2015). "Microstructural, optical and electrical transport properties of WO₃ nanoparticles coated polypyrrole hybrid nanocomposites," *Synthetic Metals* 199, 187-195. DOI: 10.1016/j.synthmet.2014.11.031
- Paralikar, S. A., Simonsen J., and Lombardi J. (2008). "Poly(vinyl alcohol)/cellulose nanocrystal barrier membranes," *Journal of Membrane Science* 320, 248-258. DOI: 10.1016/j.memsci.2008.04.009
- Ramdani, N., Wang, J., Wang, H., Feng, T. T., Derradji, M., and Liu, W. B. (2014). "Mechanical and thermal properties of silicon nitride reinforced polybenzoxazine nanocomposites," *Composites Science & Technology* 105(dec.), 73-79. DOI: 10.1016/j.compscitech.2014.10.006
- Sun, Y., Yin, Y., Mayers, B. T., Herricks, T., and Xia, Y. (2002). "Uniform silver nanowires synthesis by reducing agno₃ with ethylene glycol in the presence of seeds and poly(vinyl pyrrolidone)," *Chemistry of Materials* 14(11), 4736-4745. DOI: 10.1021/cm020587b
- Yu, H. Y., Qin, Z. Y., Sun, B., Yan, C. F., and Yao, J. M. (2013). "One-pot green fabrication and antibacterial activity of thermally stable corn-like CNC/Ag nanocomposites," *Journal of Nanoparticle Research* 16, 2202. DOI: 10.1007/s11051-013-2202-4
- Yu, H. Y., Sun, B., Zhang, D., Chen, G. Y., Yang, X. Y., and Yao, J. M. (2014a). "Reinforcement of biodegradable poly (3-hydroxybutyrate-co-3-hydroxyvalerate) with cellulose nanocrystal/silver nanohybrids as bifunctional nanofillers," *Journal of Materials Chemistry B* 2(48), 8479-8489. DOI: 10.1039/c4tb01372g
- Yu, H. Y., Chen, G. Y., Wang, Y. B., Wang, Y. B., and Yao, J. M. (2014b). "A facile one-pot route for preparing cellulose nanocrystal/zinc oxide nanohybrids with high antibacterial and photocatalytic activity," *Cellulose* 22, 261-273. DOI: 10.1007/s10570-014-0491-0
- Yu, H. Y., Yang, X. Y., Lu, F. F., Chen, G. Y., and Yao, J. M. (2015). "Fabrication of multifunctional cellulose nanocrystals/poly (lactic acid) nanocomposites with silver nanoparticles by spraying method," *Carbohydrate Polymers* 140, 209-219. DOI: 10.1016/j.carbpol.2015.12.030
- Zhang, L., Bryan, S. J., and Selao, T. T. (2022). "Sustainable citric acid production from CO₂ in an engineered cyanobacterium," *Frontiers in Microbiology* 13. DOI: 10.3389/fmicb.2022.973244
- Zhang, H., Yu, H. Y., Wang, C., and Yao, J. M. (2017). "Effect of silver contents in cellulose nanocrystal/silver nanohybrids on PHBV crystallization and property improvements," *Carbohydrate Polymers* 173, 7-16. DOI: 10.1016/j.carbpol.2017.05.064

Zhou, J., Ma, X. J., Li, J. N., and Zhu, L. Z. (2019). "Preparation and characterization of a bionanocomposite from poly (3-hydroxybutyrate-co-3-hydroxyhexanoate) and cellulose nanocrystals," *Cellulose* 26(2), 979-990. DOI: 10.1007/s10570-018-2136-1

Article submitted: July 19, 2023; Peer review completed: July 29, 2023; Revised version received and accepted: September 3, 2023; Published: September 28, 2023.

DOI: 10.15376/biores.18.4.7700-7712